Medical & Biological Engineering & Computing
https://doi.org/10.1007/s11517-020-02179-9

ORIGINAL ARTICLE

Radiogenomics model for overall survival prediction of glioblastoma

Navodini Wijethilake[1,2] · Mobarakol Islam[1,3] · Hongliang Ren[1,4]

Received: 29 July 2019 / Accepted: 15 April 2020

Abstract
Glioblastoma multiforme (GBM) is a very aggressive and infiltrative brain tumor with a high mortality rate. There are radiomic models with handcrafted features to estimate glioblastoma prognosis. In this work, we evaluate to what extent of combining genomic with radiomic features makes an impact on the prognosis of overall survival (OS) in patients with GBM. We apply a hypercolumn-based convolutional network to segment tumor regions from magnetic resonance images (MRI), extract radiomic features (geometric, shape, histogram), and fuse with gene expression profiling data to predict survival rate for each patient. Several state-of-the-art regression models such as linear regression, support vector machine, and neural network are exploited to conduct prognosis analysis. The Cancer Genome Atlas (TCGA) dataset of MRI and gene expression profiling is used in the study to observe the model performance in radiomic, genomic, and radiogenomic features. The results demonstrate that genomic data are correlated with the GBM OS prediction, and the radiogenomic model outperforms both radiomic and genomic models. We further illustrate the most significant genes, such as IL1B, KLHL4, ATP1A2, IQGAP2, and TMSL8, which contribute highly to prognosis analysis.

Keywords Brain tumor segmentation · Glioblastoma · Survival prediction · Hypercolumn · Convolutional neural network (CNN) · PixelNet.

1 Introduction

Glioblastoma multiforme (GBM) is the most reported malignant histological type. Sixteen percent of the primary brain tumors accounts for GBM [10]. Mostly they are grade IV astrocytomas. GBM-affected patients have a poor prognosis, with less than 3% survival 5 years after diagnosis [27]. Poor prognosis is a result of intra-tumor heterogeneity [23], which can be seen in levels of protein expression, metabolic behavior, or bioenergetic behavior, besides their micro-environment biochemistry and structural composition [11]. Non-invasive medical images [26] depict the entire tumor with its environment overcoming this heterogeneity. As a non-invasive medical imaging method, MRI is frequently utilized in diagnosis, prognostic analysis, and therapy or other treatment planning of patients with GBM. MRI extracts compositional, structural, functional, and physiological facts. With that information, MRI captures in vivo multidimensional portraits of GBMs, as a powerful diagnostic imaging tool [9]. Mostly manual annotation is used to segment the brain tumor in the MRI, which directs to many decision-making for treatments, other treatment planning, and overall survival calculations. However, these methods are time consuming, are tedious, and might contain human-level errors. Therefore, the necessity of automatic segmentation and survival prediction arises.

Nonetheless, these descriptors are unable to provide molecular-level data, which are heterogeneous as well. Accordingly, to overcome this constraint, the concept of radiogenomics is initiated, where we study the relationship between imaging and corresponding genomic features. Radiogenomics has the potential to predict the clinical characteristics of GBM non-invasively [13]. Remarkable

✉ Hongliang Ren
ren@nus.edu.sg; hlren@ieee.org

1 Department of Biomedical Engineering, National University of Singapore, Singapore, Singapore

2 Department of Electronics and Telecommunications, University of Moratuwa, Moratuwa, Sri Lanka

3 NUS Graduate School for Integrative Sciences and Engineering (NGS), National University of Singapore, Singapore, Singapore

4 Chinese University of Hong Kong, Hong Kong, Hong Kong

Published online: 03 June 2020

associations have connections with anatomical imaging characteristics and underlying histopathologies such as tumor cell proliferation and contrast-enhancing tumor, necrotic tissue, and hypointensity on T1-weighted images and between non-enhancing and hyperintensity on T2-weighted images.

Other attributes of GBM, which show the association between radiology and pathology, as the growth in vascular permeability, are visible through the enhancement after administration of exogenous contrast. Moreover, tumor size, location, composition, and characteristic features comprise relationships with molecular and genomic characteristics, including gene expression signatures [11]. Gene expression profiling indicates the gene expression under a particular biological condition. It can be used for pattern characterization, as the cellular status is comprehended in the gene expression profile. Verhaak et al. [39] exploit gene expression to classify GBM into four sub-types, such as proneural, neural, classical, and mesenchymal. The study clarifies that survival varies with the subtype for GBM patients. Furthermore, Kin et al. [20] identify a specific survival model for GBM integrating genomic expression data.

Recently, the deep learning approach in this field proliferated, mostly in the applications of segmentation [18], classification [36], and regression [17]. By doing segmentation, we can extract volume and shape features to do a quantitative analysis of clinical parameters [6]. Initially, convolutional neural network (CNN)–based architectures such as U-net are for segmentation [7]. Furthermore, CNN architectures are used for segmentation and extract features such as shape, histogram, and geometric features from the whole tumor and sub-regions. Later, apply machine learning approaches like random forest regression (RFR) [34], artificial neural network (ANN) [17], support vector machine (SVM) [28], linear regression (LR) [33], and gradient boosting (GB) [1] for overall survival prediction. Jungo et al. [19] have proposed a full-resolution residual convolution network for segmentation and derive geometrical features (volume, volume ratios, surface, surface irregularity, etc.) from predicting overall survival by training a fully connected neural network on four selected features.

In this study, we propose the OS prediction approach by fusing radiomic and genomic features, as shown in Fig. 1. We leverage the hypercolumn-based convolutional network inspired by multi-model PixelNet [16] and modify it to improve the performance for the segmentation of the tumor regions from MRI. We extract features such as geometric, fractal, and histogram for a selected number of regions from the segmented tumor. Subsequently, recursive feature elimination (RFE) is applied to derive the most dominant features from both gene expression and other extracted features for overall survival prediction with regression models. We utilize the TCGA dataset containing gene expression and MRI for the GBM patients, demonstrating that integrating genomic features with radiomic can boost-up the prediction accuracy of the overall survival days while identifying the most important features for the model.

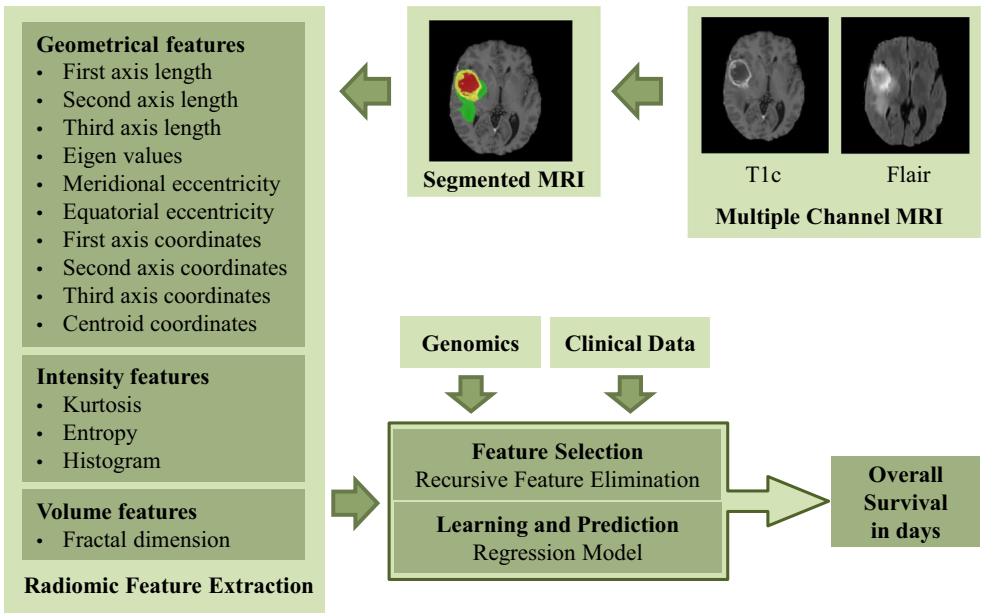

Fig. 1 Our proposed "Radiogenomic" approach overview. It fuses geometric, intensity, volumetric, genomic and clinical information to predict OS

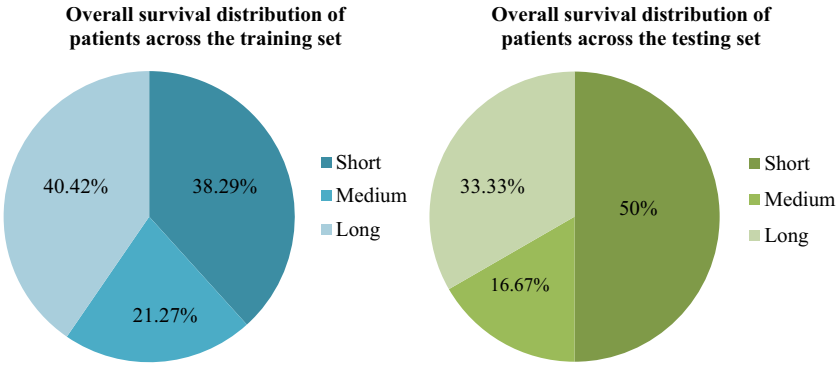

Fig. 2 The overall survival distribution of patients of our dataset. 3:1:2 ratio for short:medium:long survival is maintained in both training and testing datasets

2 Methodology

2.1 Dataset

The radiogenomic experiments of this study are conducted on The Cancer Genome Atlas (TCGA) dataset. To predict tumor regions, we train the segmentation model using The Multimodal Brain Tumor Segmentation (BraTS) 2017 data [3, 4, 25].

2.1.1 TCGA

TCGA[1] is one of the largest cancer databases consisting of imaging and genomic data. The study [39] is extracted 202 cases of gene expression profiling value from TCGA, where 59 cases of these contain MRI data. There are commonly two available modalities of flair and T1 contrast. All the MRI scans are skull-stripped and registered to 155 × 240 × 240 voxel as BraTS 2017 by using open-source software 3D slicer [31]. TCGA does not have tumor delineation. Therefore, we employ the trained model of BraTS 2017 to predict the tumor regions of the TCGA dataset.

On the other hand, there are gene expression level data of 1740 genes available for each case. Figure 3 discloses the relationship between the obtained gene expression information of the 1740 genes and the overall survival class. The dataset is divided into 47 and 12 cases for the training and validation of the OS estimation experiments. The distribution of data as short, medium, and long survival classes is in Fig. 2. The relationship between the obtained gene expression information of the 1740 genes and the overall survival class is illustrated in Fig. 3.

2.1.2 BraTS 2017

BraTS 2017 dataset is used to train our segmentation model, which is to further predict the tumor segmentation for the TCGA dataset. The dataset contains the training and validation set of 285 and 46 cases. There are four modalities of flair, t1 contrast, t1, and t2. We use flair and t1 contrast for this study as TCGA dataset those modalities only. The voxel size of each modality is 155 × 240 × 240, with isotropic voxel spacing. There are three regions, such as necrotic and non-enhancing tumor (NCR/NET-label 1), edema (ED-label 2), and enhance tumor (ET-label 4) annotated in the ground-truth.

[1] https://www.cancer.gov/tcga

2.2 Segmentation model

Our model is inspired by multimodal PixelNet [5, 16] architecture where consists of 15 convolution block as [24, 35], a hypercolumn, and a multilayer perceptron as illustrated in Fig. 4 . We have added 3 more convolution blocks with kernel size of 3 × 3 which improves the deeper level feature learning and boosts the segmentation prediction of tumor regions. As PixelNet has freedom of sampling pixel while training, hence, we choose pixels inside brain region (ignoring large MRI padding or background) which helps to minimize the class skewness. Therefore, the model consists of 18 convolutional layers (c), a hypercolumn (hp), and 3 fully connected layers (fc) such as:

$\{c_{11}, c_{12}, c_{21}, c_{22}, c_{31}, c_{32}, c_{33}, c_{42}, c_{43}, c_{51}, c_{52}, c_{53}, c_{61}, c_{62}, c_{63}, c_7, c_8, hp, fc_1, fc_2, fc_3\}$.

Convolutional features from 7 layers denoted as $\{c_{12}, c_{22}, c_{33}, c_{43}, c_{53}, c_{63}, c_7\}$ are extracted to form the hypercolumn. Only the pixels in brain region of healthy and cancerous tissues are considered the region of interest (ROI) for the model training. An ROI hypercolumn descriptor can be denoted by,

$$h_{p\_ROI} = [c_{1(p\_ROI)}, c_{2(p\_ROI)}, ..., c_{M(p\_ROI)}] \quad (1)$$

where $c_{i(p\_ROI)}$ denotes the feature vector from ith layer, and h_{p_ROI} denotes the multi-scale hypercolumn features for the pixel p. The hypercolumn vector is made of concatenating hypercolumn descriptors. Resulted hypercolumn is then fed to the multi-layer perceptron (MLP), which consists of 3 fully connected layers.

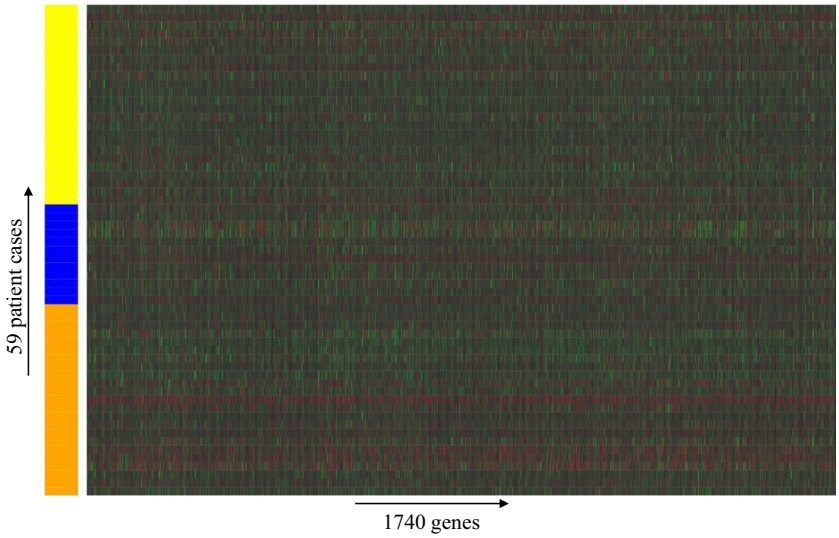

Fig. 3 Heatmap of the gene expression profiles with GBM patients. In the heatmap, the *X*-axis represents the 1740 genes, and the *Y*-axis represents the 59 patient cases. The left color bar represents the overall survival where yellow—short survival, blue—medium survival, and orange—long survival. In the heat map, the low to high gene expression levels are shown by the color gradient from green to red

2.3 Survival prediction

We extract numerous novel radiomic features from segmented tumor volume to train regression models of survival days. For example, geometric, shape, location, and histogram features are extracted from 3 regions of the tumor.

2.3.1 Feature extraction

We extract geometrical features of first axis length, second axis length, third axis length, first axis coordinates, second axis coordinates, third axis coordinates, centroid coordinates, eigenvalues, equatorial eccentricity, and meridional eccentricity, for the sub-regions of the tumor necrosis, enhanced tumor, and the whole tumor as [12, 17, 21]. The lengths and the coordinates are taken for each sub-region, as shown in Fig. 5. Eccentricity measures how much circular a certain sub-region is, while meridional eccentricity and equatorial eccentricity give the eccentricity of a section by a plane, through the longest and shortest axes and the center, perpendicular to the polar axis respectively.

On the other hand, the fractal dimension is measured to get the geometrical complexity of biological structures from the regions of necrosis and enhanced tumor. Figure 6 shows the box-counting method [38] is used to determine the fractal properties of the 3D segmented MRI.

To get texture and histogram of the selected region, kurtosis is calculated, which quantifies the non-Gaussianity of an arbitrary probability distribution of the areas of necrosis and enhanced tumor. Kurtosis can be formulated as follows [8].

$$k = \frac{E(x-\mu)^4}{\sigma^4} \tag{2}$$

where σ is the standard deviation of x, μ is the mean of x, and E is the expected value.

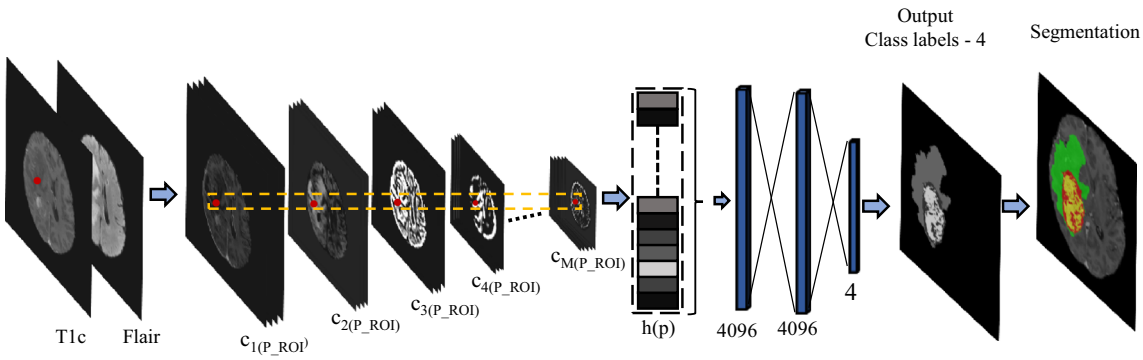

Fig. 4 Our proposed segmentation architecture. A single layer of the hypercolumn vector is made of feature descriptors from multiple convolutional layers (shown in the dashed yellow box). This hypercolumn vector propagates to the MLP for 4 class pixel-wise classification

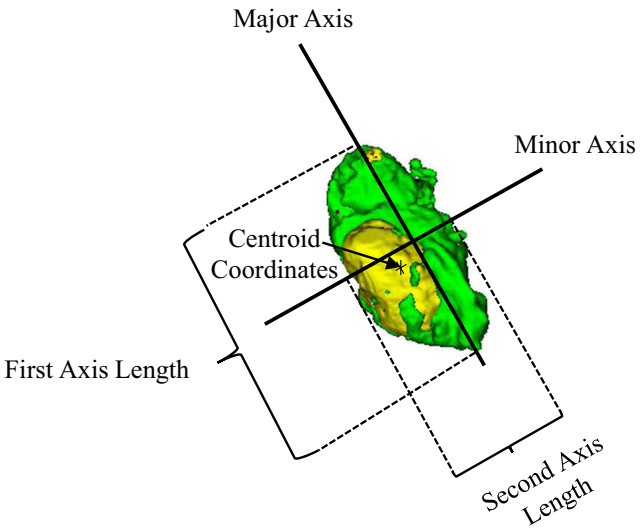

Fig. 5 Visualization of the extracted geometry features for the whole tumor sub-region, which contains necrosis, enhancement region, and edema. Red label: necrosis, yellow label: enhancement, green label: edema

Overall, we extract 96 geometric and histogram features and fuse with the clinical feature, age, and genomic features to conduct further experiments.

2.3.2 Regression model

A couple of state-of-the-art regression models are exploited in the study to estimate the survival rate by using radiomic, genomic, and radiogenomic features. These are support vector machine (SVM), linear regression (LR), artificial neural network (ANN), random forest (RF), and gradient boosting (GB). Recurrent feature elimination (RFE) [14] technique is applied to select the most important radiogenomic features, as a fusion of both radiomic and genomic features. The well-known python library *sklearn* [30] is utilized to design all the regression experiments.

3 Experiments and results

3.1 GBM segmentation

We train and validate our segmentation model with BraTS 2017 dataset. The hyper-parameters are tuned as learning rate 0.0015, momentum 0.9, and weight decay 0.0001. Pytorch [29] deep learning framework is used to conduct all the experiments.

Further, the BraTS 2017 trained model is exploited to predict the GBM region segmentation for the TCGA dataset. Table 1 shows the segmentation accuracy our models for BraTS 2017 validation dataset. Dice and Hausdorff metrics are to evaluate the regions of the tumor, such as enhanced tumor (ET), whole tumor (WT), and tumor core (TC). The performance of our model (modified PixelNet) is compared with original PixelNet [5] and well-known segmentation model UNet [32]. Our model produces better performances with most of the evaluation metrics. The predicted segmentation for BraTS 2017 and TCGA are as shown in Figs. 7 and 8 respectively.

3.2 Overall survival prediction

The most significant features selected with RFE out of radiomic, genomic, and radiogenomic features are used to train regression models of linear regression (LR), ANN, SVM, random forest (RF), and gradient boosting (GB). Fivefold cross-validation is performed to evaluate the models with the metrics of accuracy, sensitivity, and specificity. Table 2 and Fig. 9 demonstrate the performance of the radiomic, genomic, and radiogenomic model for all these models. Initially, 25 and 50 radiogenomic features, given in the Appendix, are selected with RFE for prediction and later, tuned the feature selection to obtain the best number of features that impacts the overall survival prediction.

Linear regression shows the best performance with an accuracy of 89.58% and MSE of 8324.172 for genomics. The performance of the linear regression model increases to an accuracy of 91.6% with radiomics, where the input comprises 28 genomic markers and 5 radiomic markers, altogether 33 radiogenomic features (given in the Appendix, after feature elimination. These radiomic markers consist of the centroid coordinates and fractal dimensions of the enhancement region and second axis length of the necrosis region. However, random forest regression (RFR) and gradient boosting (GB) showed a low performance compared to the other models. Table 2 shows the performance with radiogenomics for several models.

4 Discussion

We have used two normalization methods to obtain the best regression model: standardize radiomic features by scaling to unit variance and scale radiomic features individually to the unit norm and removing the mean. Normalizing by the first method gives the best results. Furthermore, adding age increases performance.

Moreover, RFE improves the performance of our model by eliminating features with a lower impact on overall survival. ANN models on selected genomics features selected radiomic features and the combination of both radiomic and genomic features gives a low mean squared error (MSE) and high accuracy for a low number of nodes in the hidden layer. Increasing the number of nodes in the

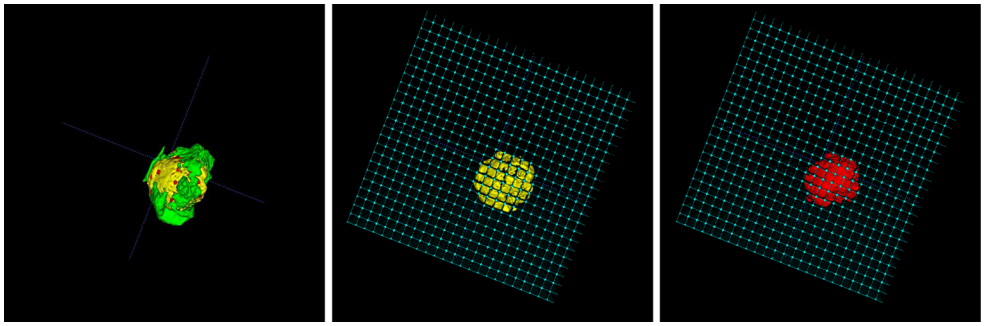

(a) (b) (c)

Fig. 6 Fractal analysis **a** 3D view of segmented MRI, **b** fractal analysis for enhanced tumor, **c** fractal analysis for necrosis. The box-counting method [38] is used to determine the fractal properties of the 3D segmented MRI. In this, we have considered up to 5 times box-count values, where the size of the box decreases each time and gives a measure

Table 1 Mean Dice score and Hausdroff distance (unit: pixels) comparison among the 3 models. *ET* enhancing tumor, *WT* whole tumor, *TC* tumor core

Model	Dice			Hausdorff		
	ET	WT	TC	ET	WT	TC
Ours	0.7035	0.8760	0.7709	7.94	7.88	9.68
PixelNet [5]	0.6971	0.8701	0.7631	7.99	7.95	10.13
UNet [32]	0.7132	0.8758	0.7516	4.67	7.91	9.70

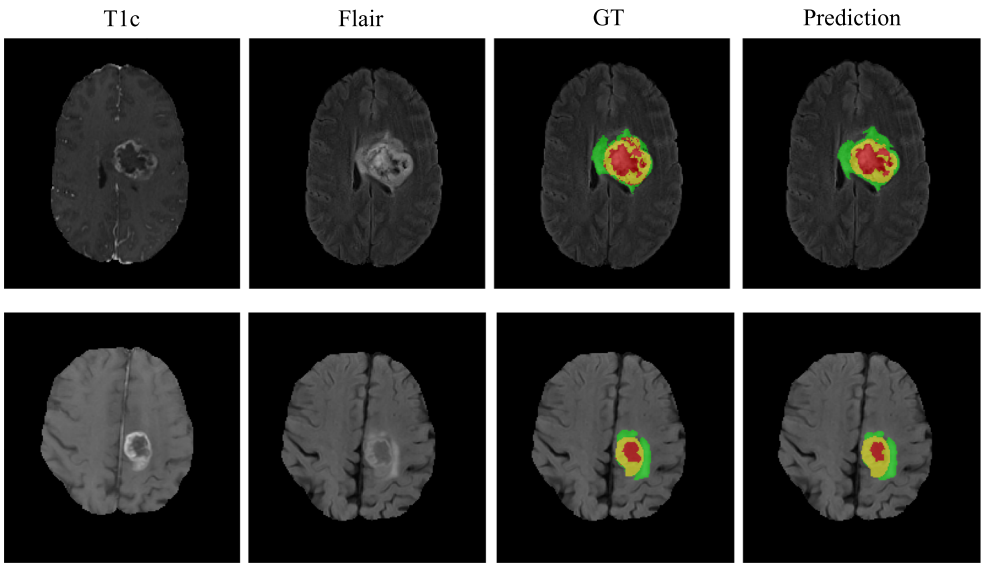

Fig. 7 Comparison of ground truth and the modified PixelNet predicted segmentation for Brats 2017 dataset. The colors red, yellow, and green denote the tumor regions, necrosis, enhanced tumor, and edema respectively

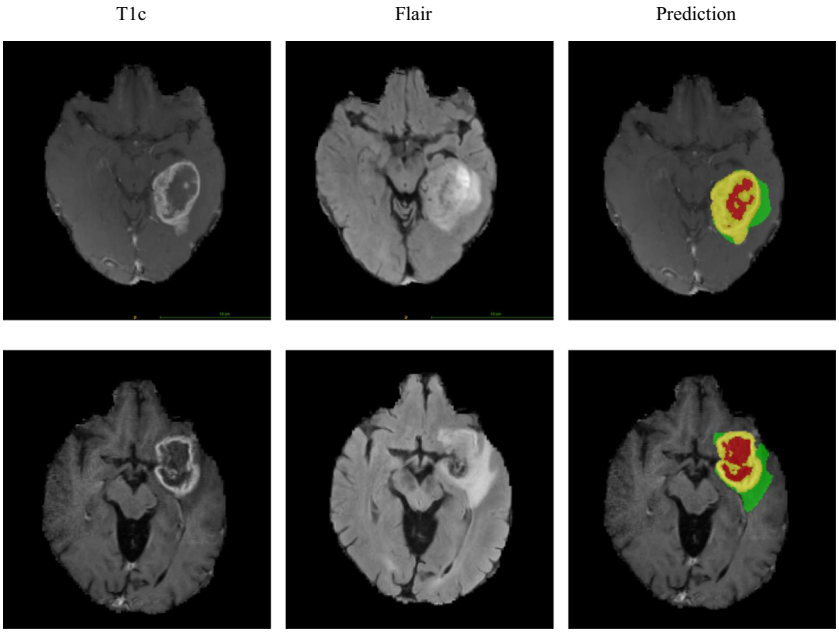

Fig. 8 Visualization of the predicted segmentation for our dataset. The model is trained for Brats 2017 dataset, and only FLAIR and T1 contrast are used

Table 2 Performance comparison of radiogenomics for different models such as ANN (artificial neural network), LR (linear regression), SVM (support vector machine), GB (gradient boosting), RFR (random forest regression), and MSE (mean squared error). Here Acc., Sens., and Spec. denote as accuracy, sensitivity, and specificity respectively.

Model		LR	SVM	ANN	RFR	GB
MSE		7576.36	12700.62	28026.79	75129.35	82734.59
Acc.		91.67%	80%	73.33%	41.67%	33.33%
Sens.	S	95%	90%	80%	16.67%	13.33%
	M	73.33%	46.66%	33.33%	66.66%	60%
	L	100%	92%	92%	75%	44%
Spec.	S	97.50%	90%	80%	78.53%	86.66%
	M	97.78%	91.11%	88.89%	84.26%	44.44%
	L	91.43%	88.57%	91.43%	51.24%	57.14%

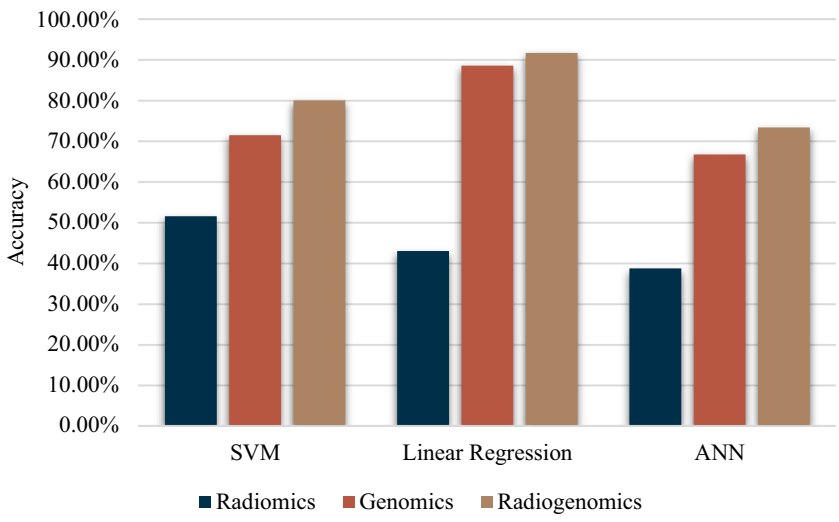

Fig. 9 Performance comparison of radiomics, genomics, and radiogenomics for the three best-performed regression models. SVM and linear regression have the best performance with RFE. However, the linear regression model gives a less mean squared error compared with SVM

hidden layer reduces accuracy and also gives a high MSE. For validating our model, we have used the Brats 2017 validation dataset. Our work is notable as we address the overall survival prediction as a regression problem other than a classification problem, which is beneficial for the clinicians to define the OS groups as they require.

In this study, we observe volume features have a high correlation with overall survival. The minimal necrosis and enhancement in GBM patients cause more prolonged survival than extensive necrosis and enhancement in GBM patients, as proved by previously done studies [15, 22]. Nevertheless, we perceive that histogram features obtained from the necrosis contribute to the prognosis of GBM patients. This further supports texture features are predictive of overall survival, as reported by Yang, Dalu et al. [40]. In addition, SHAP (SHapley Additive exPlanations) is used to explain the impact of the features for the output of the linear regression model. Figure 10 shows the most important features for the radiogenomic model, where the shap values of each feature for each patient case is graphed. This indicates that the genomic features have a higher impact on linear regression model performance and only one fradiomic feature is involved in the top 20 features. High expression values of the most significant features, i.e., KLHL4, ATP1A2, and TMSL8, increase the prediction of the model. Further, high expression values of IL1B, IQGAP2 genes have a high effect on reducing the prediction of the model.

When analyzing genomics association with prognosis, the most prominent gene is "IL1B" (interleukin-1β). This gene has been identified as a promising feature which has direct associations with GBM [37]. Our study identifies that high expression of IL1B in GBM patients have a significant impact for low overall survival in days. The other meaningful relationship from our study is the effect of the expressed TES gene for the survival of patients with GBM. It is identified as a tumor suppressor gene and as a valuable prognostic gene marker for glioblastoma [2]. Our analysis further proves that high expression of TES gene can cause for high overall survival in GBM patients.

This work has a limited dataset, which is challenging in a regression framework. In the future, the study can increase the imaging cohort by synthesizing the missing MRI modalities from the available MRI modalities. This

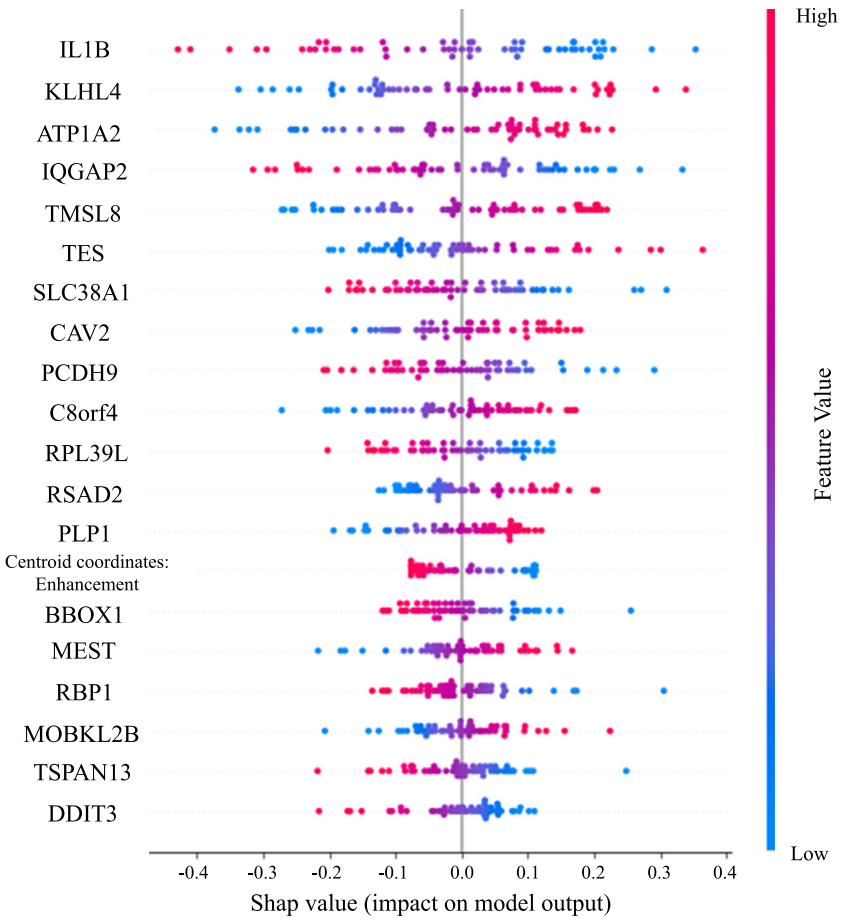

Fig. 10 Radiogenomic features explaining the linear regression model, ordered by ascending importance on the *y*-axis (each point in the summary plot represents an instance of the feature shown in the *y*-axis)

will also give a precise segmentation with more than 2 MRI modalities (T1c and Flair) as the input for the deep learning segmentation model.

5 Conclusion

In this retrospective study, we have presented a novel approach to overall survival prediction by fusing radiomic and genomic features. We have leveraged a well-known segmentation model PixelNet and modified the model to improve the prediction. We have identified that the overall survival of glioblastoma is strongly associated with both genomic and radiogenomic features. Fusing genomic expression data with radiomic features boosts up the regression accuracy of the overall survival prediction in days. This study focuses on the relationship between gene expression data together with radiomics and overall survival. Future work will focus on adding gene mutation data and deep features acquired from the MRI to enhance the performance of our model.

Funding information This work is supported by the Singapore Academic Research Fund under Grant R-397-000-297-114, and NMRC Bedside and Bench under grant R-397-000-245-511 awarded to Dr. Hongliang Ren.

Appendix

Initial 25 features selected for survival analysis:

- Centroid coordinates of enhancement region
- BBOX1
- LRAP
- TMSL8
- CAV2
- KLHL4
- TUBA4A
- PCDH9
- SLC38A1
- TSPAN13
- IQGAP2
- GBAS
- RSAD2
- MEST
- ASPN
- PLP1
- C8orf4
- RBP1
- MOBKL2B
- ECT2
- IL1B
- RPL39L
- TES
- ATP1A2
- DDIT3

Initial 25 features selected for survival analysis:

- Fractal dimensions of enhancement region
- Centroid coordiantes of enhancement region
- Second axis length of necrosis
- BBOX1
- LRAP
- TMSL8
- ALDH1L1
- SCG2
- PALMD
- CAV2
- MAPK4
- KLHL4
- COL3A1
- DIRAS3
- TUBA4A
- GSTM3
- PCDH9
- SLC38A1
- ARL4A
- TSPAN13
- EDNRA
- NEFL
- LIMS1
- D4S234E
- GABBR2
- IQGAP2
- RND3
- GBAS
- RSAD2
- MEST
- EYA4
- ATP10B
- C1QTNF3
- ASPN
- DCN
- PLP1
- C8orf4
- RBP1
- MOBKL2B
- ECT2
- GPC4
- IL1B
- RPL39L
- REV3L
- CCL20
- TES
- ECM2

- DDIT3
- FAM46A

Most important 33 features features contributed for survival analysis:

- Fractal dimensions of enhancement region
- Second axis length of necrosis
- BBOX1
- LRAP
- TMSL8
- CAV2
- ALDH1L1
- SCG2
- PALMD
- KLHL4
- TUBA4A
- PCDH9
- SLC38A1
- TSPAN13
- IQGAP2
- GBAS
- Centroid coordinates of enhancement region
- RSAD2
- MEST
- GABBR2
- ASPN
- PLP1
- C8orf4
- RBP1
- MOBKL2B
- ECT2
- IL1B
- RPL39L
- TES
- ATP1A2
- DDIT3

References

1. Alex V, Safwan M, Krishnamurthi G (2017) Automatic segmentation and overall survival prediction in gliomas using fully convolutional neural network and texture analysis. In: International MICCAI Brainlesion Workshop. Springer, pp 216–225
2. Bai Y, Zhang QG, Wang XH (2014) Downregulation of tes by hypermethylation in glioblastoma reduces cell apoptosis and predicts poor clinical outcome. European Journal of Medical Research 19(1):66
3. Bakas S, Akbari H, Sotiras A, Bilello M, Rozycki M, Kirby J, Freymann J, Farahani K, Davatzikos C (2017) Segmentation labels and radiomic features for the pre-operative scans of the tcga-gbm collection. The Cancer Imaging Archive, pp 286
4. Bakas S, Akbari H, Sotiras A, Bilello M, Rozycki M, Kirby JS, Freymann JB, Farahani K, Davatzikos C (2017) Advancing the cancer genome atlas glioma mri collections with expert segmentation labels and radiomic features. Scientific Data 4:170117
5. Bansal A, Chen X, Russell B, Gupta A, Ramanan D (2017) Pixelnet: Representation of the pixels, by the pixels, and for the pixels. arXiv:170206506
6. Bauer S, Wiest R, Nolte LP, Reyes M (2013) A survey of mri-based medical image analysis for brain tumor studies. Physics in Medicine & Biology 58(13):R97
7. Çiçek Ö, Abdulkadir A, Lienkamp SS, Brox T, Ronneberger O (2016) 3d u-net: learning dense volumetric segmentation from sparse annotation. In: International conference on medical image computing and computer-assisted intervention. Springer, pp 424–432
8. DeCarlo LT (1997) On the meaning and use of kurtosis. Psychological Methods 2(3):292
9. Diehn M, Nardini C, Wang DS, McGovern S, Jayaraman M, Liang Y, Aldape K, Cha S, Kuo MD (2008) Identification of noninvasive imaging surrogates for brain tumor gene-expression modules. Proc Natl Acad Sci 105(13):5213–5218
10. Dolecek TA, Propp JM, Stroup NE, Kruchko C (2012) Cbtrus statistical report: primary brain and central nervous system tumors diagnosed in the United States in 2005–2009. Neuro-oncology 14(suppl_5):v1–v49
11. Ellingson BM (2015) Radiogenomics and imaging phenotypes in glioblastoma: novel observations and correlation with molecular characteristics. Curr Neurol Neurosci Reports 15(1): 506
12. Farag A, Ali A, Graham J, Farag A, Elshazly S, Falk R (2011) Evaluation of geometric feature descriptors for detection and classification of lung nodules in low dose ct scans of the chest. In: 2011 IEEE International Symposium on Biomedical Imaging: from nano to macro. IEEE, Piscataway, pp 169–172
13. Gevaert O, Mitchell LA, Achrol AS, Xu J, Echegaray S, Steinberg GK, Cheshier SH, Napel S, Zaharchuk G, Plevritis SK (2014) Glioblastoma multiforme: exploratory radiogenomic analysis by using quantitative image features. Radiology 273(1):168–174
14. Guyon I, Weston J, Barnhill S, Vapnik V (2002) Gene selection for cancer classification using support vector machines. Machine Learning 46(1-3):389–422
15. Hammoud MA, Sawaya R, Shi W, Thall PF, Leeds NE (1996) Prognostic significance of preoperative mri scans in glioblastoma multiforme. J Neuro-oncology 27(1):65–73
16. Islam M, Ren H (2017) Multi-modal pixelnet for brain tumor segmentation. In: International MICCAI Brainlesion Workshop. Springer, New York, pp 298–308
17. Islam M, Jose VJM, Ren H (2018) Glioma prognosis: Segmentation of the tumor and survival prediction using shape, geometric and clinical information. In: International MICCAI Brainlesion Workshop. Springer, New York, pp 142–153
18. Islam M, Li Y, Ren H (2019) Learning where to look while tracking instruments in robot-assisted surgery. In: International Conference on Medical Image Computing and Computer-Assisted Intervention. Springer, New York, pp 412–420
19. Jungo A, McKinley R, Meier R, Knecht U, Vera L, Pérez-Beteta J, Molina-García D, Pérez-García VM, Wiest R, Reyes M (2017) Towards uncertainty-assisted brain tumor segmentation and survival prediction. In: International MICCAI Brainlesion Workshop. Springer, New York, pp 474–485
20. Kim YW, Koul D, Kim SH, Lucio-Eterovic AK, Freire PR, Yao J, Wang J, Almeida JS, Aldape K, Yung WA (2013) Identification of prognostic gene signatures of glioblastoma: a study based on tcga data analysis. Neuro-oncology 15(7):829–839

21. Ko C, Sohn G, Remmel TK (2013) Tree genera classification with geometric features from high-density airborne lidar. Can J Remote Sens 39(sup1):S73–S85
22. Lacroix M, Abi Said D, Fourney DR, Gokaslan ZL, Shi W, DeMonte F, Lang FF, McCutcheon IE, Hassenbusch SJ, Holland E et al (2001) A multivariate analysis of 416 patients with glioblastoma multiforme: prognosis, extent of resection, and survival. J Neurosurg 95(2):190–198
23. Lambin P, Rios-Velazquez E, Leijenaar R, Carvalho S, van Stiphout RG, Granton P, Zegers CM, Gillies R, Boellard R, Dekker A et al (2012) Radiomics: extracting more information from medical images using advanced feature analysis. Europ J Cancer 48(4):441–446
24. Long J, Shelhamer E, Darrell T (2015) Fully convolutional networks for semantic segmentation. In: Proceedings of the IEEE conference on computer vision and pattern recognition, pp 3431–3440
25. Menze BH, Jakab A, Bauer S, Kalpathy-Cramer J, Farahani K, Kirby J, Burren Y, Porz N, Slotboom J, Wiest R et al (2015) The multimodal brain tumor image segmentation benchmark (brats). IEEE Trans Med Imaging 34(10):1993
26. Nadeau C, Ren H, Krupa A, Dupont PE (2015) Intensity-based visual servoing for instrument and tissue tracking in 3d ultrasound volumes. IEEE Trans Autom Sci Eng 12(1):367–371. https://doi.org/10.1109/TASE.2014.2343652
27. Ohgaki H, Kleihues P (2005) Epidemiology and etiology of gliomas. Acta Neuropathologica 109(1):93–108
28. Osman AF (2017) Automated brain tumor segmentation on magnetic resonance images and patient's overall survival prediction using support vector machines. In: International MICCAI Brainlesion Workshop. Springer, New York, pp 435–449
29. Paszke A, Gross S, Chintala S, Chanan G, Yang E, DeVito Z, Lin Z, Desmaison A, Antiga L, Lerer A (2017) Automatic differentiation in pytorch. In: NIPS-W
30. Pedregosa F, Varoquaux G, Gramfort A, Michel V, Thirion B, Grisel O, Blondel M, Prettenhofer P, Weiss R, Dubourg V, Vanderplas J, Passos A, Cournapeau D, Brucher M, Perrot M, Duchesnay E (2011) Scikit-learn: Machine learning in Python. J Mach Learn. Res 12:2825–2830
31. Ren H, Vasilyev NV, Dupont PE (2011) Detection of curved robots using 3d ultrasound. In: IROS 2011, IEEE/RSJ International Conference on Intelligent Robots and Systems. https://doi.org/10.1109/IROS.2011.6094915, pp 2083–2089
32. Ronneberger O, Fischer P, Brox T (2015) U-net: Convolutional networks for biomedical image segmentation. In: International Conference on Medical image computing and computer-assisted intervention. Springer, New York, pp 234–241
33. Saffari SE, Löve Á, Fredrikson M, Smedby Ö (2015) Regression models for analyzing radiological visual grading studies–an empirical comparison. BMC Med Imaging 15(1):49
34. Shboul ZA, Vidyaratne L, Alam M, Iftekharuddin KM (2017) Glioblastoma and survival prediction. In: International MICCAI Brainlesion Workshop. Springer, New York, pp 358–368
35. Simonyan K, Zisserman A (2014) Very deep convolutional networks for large-scale image recognition. arXiv:14091556
36. Srinivasan VB, Islam M, Zhang W, Ren H (2018) Finger movement classification from myoelectric signals using convolutional neural networks. In: 2018 IEEE International Conference on Robotics and Biomimetics(ROBIO). IEEE, Piscataway, pp 1070–1075
37. Tarassishin L, Casper D, Lee SC (2014) Aberrant expression of interleukin-1β and inflammasome activation in human malignant gliomas. PloS one 9(7)
38. Theiler J (1990) Estimating fractal dimension. JOSA A 7(6):1055–1073
39. Verhaak RG, Hoadley KA, Purdom E, Wang V, Qi Y, Wilkerson MD, Miller CR, Ding L, Golub T, Mesirov JP et al (2010) Integrated genomic analysis identifies clinically relevant subtypes of glioblastoma characterized by abnormalities in pdgfra, idh1, egfr, and nf1. Cancer Cell 17(1):98–110
40. Yang D, Rao G, Martinez J, Veeraraghavan A, Rao A (2015) Evaluation of tumor-derived mri-texture features for discrimination of molecular subtypes and prediction of 12-month survival status in glioblastoma. Med Phys 42(11):6725–6735

Navodini Wijethilake is a Bsc Engineering undergraduate of University of Moratuwa, Sri Lanka. She worked as a research intern at Medical Mechatronics lab at National University of Singapore.

Mobarakol Islam is currently pursuing PhD from National University of Singapore, Singapore. His current research interests are in the field of deep learning, medical imaging and image-guided surgery.

Hongliang Ren is currently leading a research group on medical mechatronics in the Biomedical Engineering Department of National University of Singapore (NUS). He is an affiliated Principal Investigator for the Singapore Institute of Neurotechnology (SINAPSE), NUS (Suzhou) Research Institute, and Advanced Robotics Center at National University of Singapore (NUS). Dr. Ren received his Ph.D. in Electronic Engineering (Specialized in Biomedical Engineering) from The Chinese University of Hong Kong (CUHK) in 2008. Prior to joining NUS, he was a Research Fellow at The Johns Hopkins University, Children's Hospital Boston & Harvard Medical School, and Children's National Medical Center, USA. His main areas of interest include Biorobotics & Intelligent Control, Medical Mechatronics, Computer-Integrated Surgery, and Multisensor Data Fusion in Surgical Robotics. Dr. Ren is IEEE Senior Member and currently serves as Associate Editor for IEEE Transactions on Automation Science & Engineering (T-ASE) and Medical & Biological Engineering & Computing (MBEC). He is the recipient of NUS Young Investigator Award, IAMBE Early Career Award 2018 & Interstellar Early Career Investigator Award 2018.